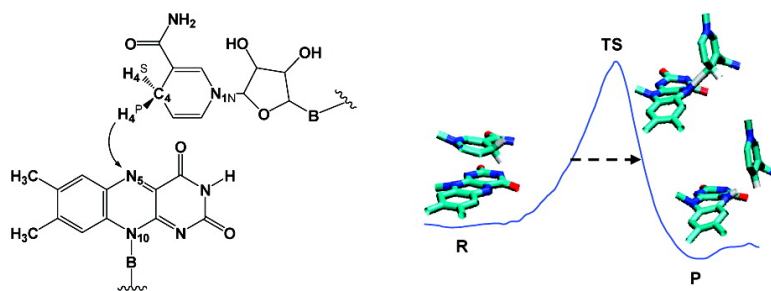Article

Deep Tunneling Dominates the Biologically Important Hydride Transfer Reaction from NADH to FMN in Morphinone Reductase

Jiayun Pang, Sam Hay, Nigel S. Scrutton, and Michael J. Sutcliffe

More About This Article

Additional resources and features associated with this article are available within the HTML version:

- Supporting Information
- Links to the 6 articles that cite this article, as of the time of this article download
- Access to high resolution figures
- Links to articles and content related to this article
- Copyright permission to reproduce figures and/or text from this article

View the Full Text HTML

Deep Tunneling Dominates the Biologically Important Hydride Transfer Reaction from NADH to FMN in Morphinone Reductase

Jiayun Pang,[†] Sam Hay,[‡] Nigel S. Scrutton,[‡] and Michael J. Sutcliffe*,[†]

Manchester Interdisciplinary Biocentre, School of Chemical Engineering and Analytical Science, and Faculty of Life Sciences, University of Manchester, 131 Princess Street, Manchester M1 7DN, U.K.

Received January 23, 2008; E-mail: mike.sutcliffe@manchester.ac.uk

Abstract: The temperature dependence of the primary kinetic isotope effect (KIE), combined temperature−pressure studies of the primary KIE, and studies of the α-secondary KIE previously led us to infer that hydride transfer from nicotinamide adenine dinucleotide to flavin mononucleotide in morphinone reductase proceeds via environmentally coupled hydride tunneling. We present here a computational analysis of this hydride transfer reaction using QM/MM molecular dynamics simulations and variational transition-state theory calculations. Our calculated primary and secondary KIEs are in good agreement with the corresponding experimental values. Although the experimentally observed KIE lies below the semiclassical limit, our calculations suggest that ∼99% of the reaction proceeds via tunneling: this is the first "deep tunneling" reaction observed for hydride transfer. We also show that the dominant tunneling mechanism is controlled by the isotope at the primary rather than the secondary position: with protium in the primary position, large-curvature tunneling dominates, whereas with deuterium in this position, small-curvature tunneling dominates. Also, our study is consistent with tunneling being preceded by reorganization: in the reactant, the rings of the nicotinamide and isoalloxazine moieties are stacked roughly parallel to each other, and as the system moves toward a "tunneling-ready" configuration, the nicotinamide ring rotates to become almost perpendicular to the isoalloxazine ring.

Introduction

Evidence for environmentally coupled H tunneling in enzyme systems is gleaned from experimental studies employing isotopic substitution of the transferred [primary (1°)] or neighboring [secondary (2°)] H nucleus.[1] Computational studies provide essential atomistic insight into the mechanism of H transfer.[2] Agreement between experiment, computation, and theory provides powerful evidence in support of environmentally coupled H tunneling.[1,3,4] Computational simulations have indicated that in a number of enzyme systems, H transfer can occur by a mixture of "over the barrier" and "through the barrier" events;[2,4–8] in only a few systems is transfer essentially a "pure" tunneling process,[2,9,10] that is, a so-called "deep tunneling" reaction. Simulation has revealed a major role for dynamics in the H-transfer event, in terms of both (1) a collective, thermally equilibrated motion to attain degenerate quantum states of the reactants and products[11] and (2) a fast, nonequilibrated "promoting" motion that modifies the properties of the tunneling barrier once the degenerate states have been reached.[9,12] The existence of promoting motions has been contentious.[9,13] However, combined studies embracing experiment, simulation, and numerical analysis have supported the existence of promoting motions in enzyme systems.[14–18]

(1) Kohen, A. In *Hydrogen Transfer Reactions*; Hynes, J. T., Klinman, J. P., Limbach, H. H., Schowen, R. L., Eds.; Wiley: Weinheim, Germany, 2006; Vol. 4, pp 1311−1340.
(2) Pu, J.; Gao, J.; Truhlar, D. G. *Chem. Rev.* **2006**, *106*, 3140–3169.
(3) Sutcliffe, M. J.; Scrutton, N. S. *Phys. Chem. Chem. Phys.* **2006**, *8*, 4510–4516.
(4) Hammes-Schiffer, S. *Acc. Chem. Res.* **2006**, *39*, 93–100.
(5) Pang, J.; Pu, J.; Gao, J.; Truhlar, D. G.; Allemann, R. K. *J. Am. Chem. Soc.* **2006**, *128*, 8015–8023.
(6) Alhambra, C.; Corchado, J.; Sanchez, M. L.; Garcia-Viloca, M.; Gao, J.; Truhlar, D. G. *J. Phys. Chem. B* **2001**, *105*, 11326–11340.
(7) Billeter, S. R.; Webb, S. P.; Agarwal, P. K.; Iordanov, T.; Hammes-Schiffer, S. *J. Am. Chem. Soc.* **2001**, *123*, 11262–11272.
(8) Cui, Q.; Karplus, M. *J. Am. Chem. Soc.* **2002**, *124*, 3093–3124.
(9) Masgrau, L.; Roujeinikova, A.; Johannissen, L. O.; Hothi, P.; Basran, J.; Ranaghan, K. E.; Mulholland, A. J.; Sutcliffe, M. J.; Scrutton, N. S.; Leys, D. *Science* **2006**, *312*, 237–241.
(10) Tejero, I.; Garcia-Viloca, M.; Gonzalez-Lafont, A.; Lluch, J. M.; York, D. M. *J. Phys. Chem. B* **2006**, *110*, 24708–24719.
(11) Benkovic, S. J.; Hammes-Schiffer, S. *Science* **2003**, *301*, 1196–1202.
(12) Caratzoulas, S.; Mincer, J. S.; Schwartz, S. D. *J. Am. Chem. Soc.* **2002**, *124*, 3270–3276.
(13) Ball, P. *Nature* **2004**, *431*, 396–397.
(14) Johannissen, L. O.; Hay, S.; Scrutton, N. S.; Sutcliffe, M. J. *J. Phys. Chem. B* **2007**, *111*, 2631–2638.
(15) Hay, S.; Sutcliffe, M. J.; Scrutton, N. S. *Proc. Natl. Acad. Sci. U.S.A.* **2007**, *104*, 507–512.
(16) Agarwal, P. K.; Billeter, S. R.; Hammes-Schiffer, S. *J. Phys. Chem. B* **2002**, *106*, 3283–3293.
(17) Garcia-Viloca, M.; Truhlar, D. G.; Gao, J. *Biochemistry* **2003**, *42*, 13558–13575.
(18) Dybala-Defratyka, A.; Paneth, P.; Banerjee, R.; Truhlar, D. G. *Proc. Natl. Acad. Sci. U.S.A.* **2007**, *104*, 10774–10779.

In developing an interdisciplinary program embracing computation, theory, and experiment, we have extensively studied the hydride-transfer reaction from nicotinamide adenine dinucleotide (NADH) to enzyme-bound flavin mononucleotide (FMN) in the flavoprotein morphinone reductase (MR). We inferred that this reaction proceeds via environmentally coupled hydride tunneling on the basis of studies of the temperature dependence of the 1° kinetic isotope effect (KIE),[19,20] combined temperature−pressure studies of the 1° KIE,[15] and studies of the α-secondary (α-2°) KIE.[20]

In the present study, we report the first computational simulation of the hydride transfer reaction from NADH to FMN in MR. This represents an important, widespread class of reactions in biology. We show remarkable agreement between experiment and simulation for the magnitudes of both the 1° and 2° KIEs. Our simulations reveal that in contrast to other systems involving hydride transfer that have been studied,[5,7] hydride transfer in MR occurs almost entirely by H tunneling. Remarkably, we show that the tunneling mechanism is dependent on the nature of the isotopic label, changing from a large-curvature tunneling regime in the case of hydride transfer to a small-curvature tunneling regime for deuteride transfer. Our work demonstrates the effectiveness of combining experiment and simulation in order to obtain a detailed mechanistic picture of tunneling reactions in enzymes.

Methods

The calculations were based on the crystal structure of MR with FMN and 1,4,5,6-tetrahydro-NADH (NADH$_4$) (PDB accession code 2R14),[21] with NADH$_4$ modified to NADH. The MR−FMN−NADH complex was solvated with a previously equilibrated rectangular water box and neutralized. The ionizable residues were modeled in the protonation state corresponding to pH 7 obtained using H++ (http://biophysics.cs.vt.edu/H++),[22,23] a web-based system that computes pK values of ionizable groups in enzymes. The total number of atoms resulting from this process was 33,671, of which a set of 58 atoms (28 from FMN and 30 from NADH) was treated as the quantum-mechanical (QM) region and the rest of the system as the molecular-mechanical (MM) region. The boundary between the QM and MM subsystems was defined using the generalized boundary orbital (GHO) method.[24] The AM1[25] semiempirical method was used to describe the QM subsystem. While use of such a semiempirical method could have limitations, it has been shown to describe the structure of the isoalloxazine ring in FMN as faithfully as the B3LYP method and to give reasonable results for the electron- and proton-addition reactions in the gas phase.[26] A simple valence bond (SVB) term was added in order to correct the energies at the critical points on the potential energy surface.[27] This correction included two Morse terms, which corrected the error in the difference of the heterolytic bond-dissociation energies for the two hydride-transfer half-reactions. The SVB parameter values used

for the bond-breaking (H donor) and bond-forming (H acceptor) half-reactions, respectively, were equilibrium bond lengths (r_i) of 1.101 and 1.012 Å; potential energies (D_i) of 245.7 and 214.1 kcal mol^{-1}; and, for the parameter controlling the width of the potential well for the breaking bond (α), values of 0.4 and 0.5 Å^{-1}. The coupling constant, V_{12}, was set as 23 kcal mol^{-1}. These parameters were employed on the basis of previous studies,[17] high-level gas-phase QM calculations at the B3LYP/6−311G* and HF/6−31G** levels, and trials of QM/MM umbrella samplings to reproduce the experimental free energies of reaction and activation (with estimates of the quantum and dynamical corrections added to the height of the activation barrier). The CHARMM27 force field[28] was used to present the protein and TIP3P model for water. All of the calculations employed periodic boundary conditions.

Prior to the dynamics calculations, the system was minimized using the adopted-basis Newton−Raphson (ABNR) method until the norm of the gradient was less than 10^{-3} kcal mol^{-1} Å^{-1}. Then the system was gradually heated to 298.15 K and equilibrated for a further 60 ps. A cutoff distance of 12 Å was used for the nonbonded interactions, with a switch function in the region 11−12 Å to feather the interaction energy to zero. In the subsequent calculations of the classical mechanical potential of mean force (CM-PMF) by umbrella sampling, the reaction coordinate (z) was defined geometrically as the difference between the lengths of the breaking bond (C4$_{NADH}$−H4) and the forming bond (H4−N5$_{FMN}$) involved in the hydrogen transfer. The CM-PMF is independent of mass and therefore equally applicable to all isotopomers. To obtain the CM-PMF, a total of 45 windows spanning the entire range of z were defined, with a force constant in the range 120−180 kcal mol^{-1} Å^{-2} for the harmonic restraint on z. The simulations started from the reactant state. Each window was equilibrated for 20 ps and then subjected to a 40 ps production simulation that collected the probability density of configurations (P) along z. The total simulation time was approximately 2.7 ns. The CM-PMF curves were obtained using the weighted histogram analysis method.[29]

Tunneling was modeled using ensemble-averaged variational transition-state theory with multidimensional tunneling (EA-VTST/MT) calculations[6,30−32] available via the CHARMMRATE[33] module (the interface between CHARMM and POLYRATE[34]) in CHARMM and employing LCG4[35] in the large-curvature tunneling calculations in order to compute tunneling into all available excited states. Quantized vibrational corrections to the computed CM-PMF were obtained using instantaneous normal-mode analysis of the 40-atom primary zone in the 58-atom QM region (see Figure 1). Along the umbrella-sampling path, 3600 conformations were selected. Four different isotopically substituted cases were investigated in order to determine the primary and secondary KIEs: (1) protium atoms at the H4^P and H4^S positions of the nicotinamide ring (denoted HH); (2) replacement of the protium atom at position H4^P (the transferred hydrogen) by a deuterium atom (denoted DH) to calculate the primary KIE; (3) replacement of protium by deuterium at position H4^S (denoted HD) to calculate the secondary KIE; and (4) deuterium replacement at both H4^P and H4^S (denoted DD) to calculate the double KIE.

(19) Basran, J.; Harris, R. J.; Sutcliffe, M. J.; Scrutton, N. S. *J. Biol. Chem.* **2003**, *278*, 43973–43982.

(20) Pudney, C. R.; Hay, S.; Sutcliffe, M. J.; Scrutton, N. S. *J. Am. Chem. Soc.* **2006**, *128*, 14053–14058.

(21) Pudney, C. R.; Hay, S.; Pang, J.; Costello, C.; Leys, D.; Sutcliffe, M. J.; Scrutton, N. S. *J. Am. Chem. Soc.* **2007**, *129*, 13949–13956.

(22) Gordon, J. C.; Myers, J. B.; Folta, T.; Shoja, V.; Heath, L. S.; Onufriev, A. *Nucleic Acids Res.* **2005**, *33*, W368–W371.

(23) Bashford, D.; Karplus, M. *Biochemistry* **1990**, *29*, 10219–10225.

(24) Gao, J. L.; Amara, P.; Alhambra, C.; Field, M. J. *J. Phys. Chem. A* **1998**, *102*, 4714–4721.

(25) Dewar, M. J. S.; Zoebisch, E. G.; Healy, E. F.; Stewart, J. J. P. *J. Am. Chem. Soc.* **1985**, *107*, 3902–3909.

(26) Bhattacharyya, S.; Stankovich, M. T.; Truhlar, D. G.; Gao, J. *J. Phys. Chem. A* **2007**, *111*, 5729–5742.

(27) Devi-Kesavan, L. S.; Gao, J. *J. Am. Chem. Soc.* **2003**, *125*, 1532–1540.

(28) MacKerell, A. D.; et al. *J. Phys. Chem. B* **1998**, *102*, 3586–3616.

(29) Bartels, C.; Karplus, M. *J. Comput. Chem.* **1997**, *18*, 1450–1462.

(30) Truhlar, D. G.; Isaacson, A. D.; Garret, B. C. In *Theory of Chemical Reaction Dynamics*; Baer, M., Ed.; CRC Press: Boca Raton, FL, 1985; Vol. IV, p 65−136..

(31) Gao, J.; Truhlar, D. G. *Annu. Rev. Phys. Chem.* **2002**, 467–505.

(32) Truhlar, D. G.; Gao, J. L.; Garcia-Viloca, M.; Alhambra, C.; Corchado, J.; Sanchez, M. L.; Poulsen, T. D. *Int. J. Quantum Chem.* **2004**, *100*, 1136–1152.

(33) Garcia-Viloca, M.; Alhambra, C.; Corchado, J. C.; Sanchez, M. L.; Villa, J.; Gao, J.; Truhlar, D. G.; 2.0 ed.; University of Minnesota, Minneapolis: 2002.

(34) Corchado, J. C.; et al. POLYRATE, version 9.0; University of Minnesota: Minneapolis, MN, 2002.

(35) Fernandez-Ramos, A.; Truhlar, D. G. *J. Chem. Phys.* **2001**, *114*, 1491–1496.
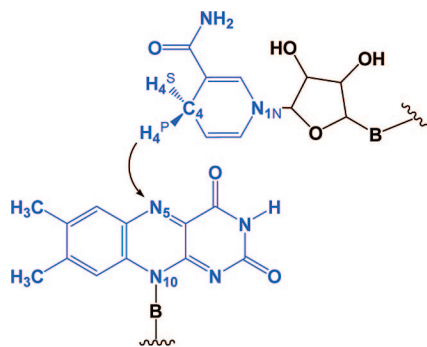
Figure 1. Schematic representation of (bottom) FMN and (top) NADH. Atoms treated at the QM level in the combined QM/MM potential energy surface are shown, with those contained in the primary zone (used to calculate quantized vibrational corrections and transmission coefficients) colored in blue. The two boundary (sp^3) carbon atoms are denoted "B".

To calculate the transmission coefficients, 12 configurations having z values in the range $z^* \pm 0.01$ Å (where z^* is the location of the transition state identified from the CM-PMF) were selected as the transition-state ensemble (TSE). For each configuration in the TSE, the atomic positions of the secondary-zone atoms were fixed, and the coordinates of the 40 atoms in the primary zone were optimized to the nearest saddle points. The isoinertial minimum-energy path (MEP) was then calculated for this saddle point, and each configuration of the TSE was used to generate a different MEP. As each MEP had a different set of coordinates for the secondary zone, the whole protein and solvent contributed to calculations of the transmission coefficients. The transmission coefficient (γ) comprises two factors, κ and Γ, where Γ accounts for the correction to the rate constant from dynamical recrossing and κ accounts for quantum-mechanical effects on the motion along the reaction coordinate (primarily tunneling but also nonclassical reflection). The product of the two factors gives the transmission coefficient for configuration i as $\gamma_i = \kappa_i \Gamma_i$.

The fraction of the reaction that proceeds by tunneling can be estimated as $(k^{\text{EA-VTST/MT}} - k^{\text{QC}})/k^{\text{QC}}$, where $k^{\text{EA-VTST/MT}}$ is the final rate constant including quantized vibrational corrections and the transmission coefficient and k^{QC} is the quasi-classical rate constant, which neglects the contribution from the tunneling factor κ. This estimated fraction of the reaction that proceeds by tunneling corresponds to a lower limit, since κ includes the effects of both tunneling and nonclassical reflection.

Results

Tunneling was investigated by simulating the free-energy profile, which was obtained by initially calculating the CM-PMF (Figure 2 and Table 1) along the predefined reaction coordinate, z, and then incorporating zero-point energy, quantum-mechanical tunneling effects, and barrier recrossing into the CM-PMF using EA-VTST/MT calculations[36] (Table 1). To include the effects of isotopic substitution into the rate-constant calculations, four different isotopically labeled forms of NADH were used, each having either H or D at the 1° (C4-R) and 2° (C4-S) positions (denoted H_4^P and H_4^S, respectively, in Figure 1); these forms are denoted as HH, DH, HD, and DD, with the first letter corresponding to the atom at the 1° position and the second to that at the 2° position. Inclusion of quantized vibrational energies lowers the free energy of activation by ~1.6 and ~0.7 kcal mol^{-1} for H and D, respectively, in the 1° position, while the free energy is relatively insensitive to the isotope in the 2° position (Table 1).
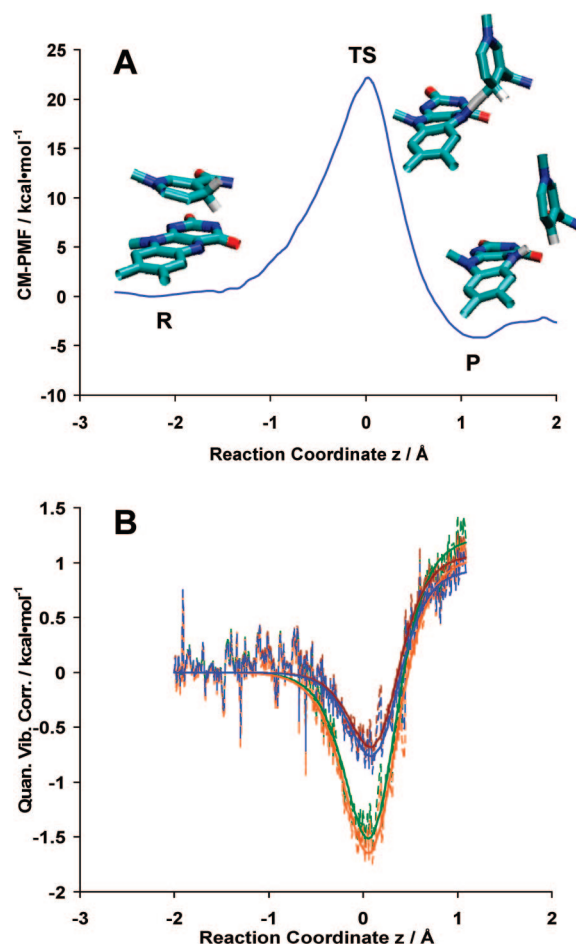
(36) Truhlar, D. G.; Gao, J.; Garcia-Viloca, M.; Alhambra, C.; Corchado, J.; Sanchez, M. L.; Poulsen, T. D. *Int. J. Quantum Chem.* **2004**, *100*, 1136–1152.

Figure 2. Free energy of activation. (A) Computed CM-PMF with representative relative configurations of FMN and NAD(H) displayed in the reactant (R), transition-state (TS), and product (P) regions. For clarity, only the isoalloxazine moiety of FMN and the nicotinamide moiety of NAD(H) are shown. (B) Quantized vibrational-energy corrections to the classical-mechanical free energy of activation. The raw data for HH, DH, HD, and DD are shown using green, brown, orange, and blue dots, respectively. These initial data were fit to an Eckart function to obtain the respective smooth lines shown.

To obtain rate constants, transmission coefficients accounting for multidimensional tunneling (κ) and dynamical recrossing (Γ) were determined and multiplied to give the overall ensemble-averaged transmission coefficient, γ (Table S1 in the Supporting Information). Large variations were observed across configurations, reflecting the fact that the tunneling probabilities are sensitive to the geometry in the TSE. Nevertheless, as would be expected, HH [with an average κ value of 350 ± 240 obtained using microcanonically optimized multidimensional tunneling (μOMT)] exhibits the highest probability of tunneling for every configuration, followed by HD (220 ± 140) and DH (90 ± 40), with DD having the lowest tunneling probability (70 ± 30). Since Γ is essentially independent of isotope (Table S1 in the Supporting Information), $\kappa^{\mu\text{OMT}}$ decreases the overall free energy of activation by 3.3, 3.0, 2.6, and 2.4 kcal mol^{-1} for HH, HD, DH, and DD, respectively. The final computed rate constants averaged over the TSE, $k^{\text{EA-VTST/MT}}$ (which are the rate constants obtained from the quasi-thermodynamic free energy of activation, $\Delta G_{\text{act},T}^{(1)}$, multiplied by the transmission coefficient, γ) are within an order of magnitude of the experimental values (Table 1). The calculated 1° KIE of 15 ± 4 (Table 1 and Table S2 in the Supporting Information) is slightly greater than the experi-

Table 1. Computed Free Energies of Activation, Reaction Rate Constants, and 1° (k^{HH}/k^{DH}), 2° (k^{HH}/k^{HD}), and Double (k^{HH}/k^{DD}) KIEs at 25 °C

	ΔG (kcal mol^{-1})			k (s^{-1})		KIE	
	$\Delta G_{R,T,F}^{CM}$ [a]	$\Delta G_{act,T}^{(1)}$ [b]	$\Delta G_{act,T}$ [c]	EA-VTST/MT	experimental[d]	calculated	experimental[d]
HH	20.60	19.09	15.8	17.7	56.4		
DH	20.64	19.97	17.4	1.05	12.2	15.4	4.6
HD	20.60	18.96	15.9	14.1	47.9	1.22	1.18
DD	20.64	19.90	17.5	0.98	10.5	16.6	5.4

[a] Classical free energy of activation corrected for the loss of free energy of the reactive normal mode[54] (the uncorrected value is 22.15 kcal mol^{-1}). [b] Free energy of activation after addition of quantized nuclear vibrational corrections. [c] Final phenomenological free energy of activation after inclusion of the effects of tunneling and barrier recrossing. [d] Values from ref 20 corrected for isotopic contamination.

mentally determined value of 4.6 (Table 1). κ decreases the overall free energy of activation by 3.27 kcal mol^{-1} for HH and 3.02 kcal mol^{-1} for HD. This difference of 0.25 kcal mol^{-1} is counterbalanced by the greater contribution of quantized vibrational energy to HD than to HH (0.13 kcal mol^{-1}) (Figure 2B). This leads to a computed 2° KIE of 1.22 ± 0.08 (Table S2 in the Supporting Information), which is in excellent agreement with the experimental value of 1.18.[20]

At the starting point for umbrella sampling (as in the crystal structure), the rings of the nicotinamide moiety of NADH and the isoalloxazine moiety of FMN are stacked parallel to each other with C4 of NADH and N5 of FMN in close proximity. As the reaction coordinate, z, increases (i.e., as the system moves along the geometrically defined reaction path from reactants to products), the distance between the hydrogen donor (C4 of NADH) and the acceptor (N5 of FMN) decreases from 4.4 ± 0.1 Å in the reactants to 2.7 ± 0.07 Å in the transition state (TS). Concomitantly, the distance between N1N of NADH and N10 of FMN increases from 5.5 ± 0.4 Å in the reactants to 6.6 ± 0.2 Å in the TS; this results in rotation of the nicotinamide ring, causing it to become almost perpendicular to the isoalloxazine ring of FMN at the TS (Figure 2A).

Our results suggest that >99% of hydride transfer occurs via tunneling (Table S1 in the Supporting Information) and that, prior to tunneling, the reacting moieties approach through heavy-atom motion (Figure 3). In the respective representative structure for tunneling, the tunneling distance for HH is 0.41 ± 0.02 Å ($s = -0.31 ± 0.03$ bohr amu$^{1/2}$, where s is the mass-weighted distance along z from the TS, with $s = 0$ at the top of the barrier and $s < 0$ on the reactant side), which falls to 0.38 Å ± 0.02 ($s = -0.38 ± 0.03$ bohr amu$^{1/2}$) for DH; when the 2° position is deuterated, the tunneling distance decreases marginally, to 0.40 ± 0.03 Å ($s = -0.36 ± 0.04$ bohr amu$^{1/2}$) for HD and 0.37 ± 0.03 Å ($s = -0.36 ± 0.05$ bohr amu$^{1/2}$) for DD.

Discussion

Free Energies. The quantized vibrational energies are slightly higher when the 2° H is replaced by deuterium: there is a 0.13 kcal mol^{-1} increase for HD relative to HH and a 0.08 kcal/mol increase for DD relative to DH. This suggests that the vibrational modes involving the 2° H may be coupled to other degree(s) of freedom in the primary zone (Figure 2B): although the vibrational frequency of the C−H4^S bond is expected to decrease when the 2° H is replaced by D, coupling with other degree(s) of freedom would lead to an increase in the overall quantized energy. In view of the sensitive nature of 2° KIEs, this slight difference in the energies of HH and HD could have a substantial impact on the computed 2° KIEs. Furthermore, it has been suggested[37] that 2° KIEs increase when there is vibrational coupling between the 2° H and the reaction coordinate. Our results suggest that this may be the case in MR. However, they

are not likely to be too closely coupled, as this would lead to a breakdown of the rule of the geometric mean, which would be at odds with experiment.[20]

Analysis of the Tunneling Path. The tunneling factor κ was obtained using μOMT method,[38] which calculates the κ value by optimizing the tunneling path between the paths of small-curvature tunneling (SCT)[39,40] and large-curvature tunneling (LCT).[41,42] SCT includes in the reaction path mild corner-cutting of the minimum-tunneling path (MEP), while in LCT, straight-line motion leads to the shortest path, with maximized corner-cutting. For comparison, the zero-curvature tunneling (ZCT) path, which neglects curvature of the reaction path (i.e., tunneling proceeds along the MEP) was also computed. The fact that the ZCT method yields a significantly smaller κ value than SCT and LCT approaches indicates that other degree(s) of freedom beyond the progress coordinate of the hydrogen participate in the tunneling path, which may be indicative of some gating motion. In addition, because the μOMT method variationally selects from the SCT and LCT paths, it increases the calculated κ value compared with those obtained using SCT and LCT (see Table S3 in the Supporting Information). For the HH isotopic form, the tunneling in 10 of the 12 configurations in the TSE proceeded via the LCT path, i.e., LCT is the dominant tunneling mechanism at the representative tunneling energy (RTE), i.e., the energy at which the probability of tunneling is greatest. In the case of HD, the number of configurations tunneling via LCT decreased to 8. When the 1° H was replaced by D, the dominant tunneling mechanism at the RTE was SCT, with all 12 configurations for DH and 11 configurations for DD following this path. This is consistent with H in the 1° position taking greater advantage of corner-cutting (i.e., LCT dominates) than does D (for which SCT dominates).[18] Thus, the isotope at the 1° position impacts substantially on the dominant tunneling mechanism, whereas the effect of isotopic substitution at the 2° position is much less pronounced.

A key element in the LCT approximation is that, this method involves convolution of the probability of a given nuclear configuration and the tunneling probability at that configuration

(37) Huskey, W. P.; Schowen, R. L. *J. Am. Chem. Soc.* **1983**, *105*, 5704–5706.
(38) Liu, Y. P.; Lu, D. H.; Gonzalez-Lafont, A.; Truhlar, D. G.; Garrett, B. C. *J. Am. Chem. Soc.* **1993**, *115*, 7806–7817.
(39) Liu, Y. P.; Lynch, G. C.; Truong, T. N.; Lu, D. H.; Truhlar, D. G.; Garrett, B. C. *J. Am. Chem. Soc.* **1993**, *115*, 2408–2415.
(40) Lu, D. H.; Truong, T. N.; Melissas, V. S.; Lynch, G. C.; Liu, Y. P.; Garrett, B. C.; Steckler, R.; Isaacson, A. D.; Rai, S. N.; Hancock, G. C.; Lauderdale, J. G.; Joseph, T.; Truhlar, D. G. *Comput. Phys. Commun.* **1992**, *71*, 235–262.
(41) Garrett, B. C.; Truhlar, D. G.; Wagner, A. F.; Dunning, T. H. *J. Chem. Phys.* **1983**, *78*, 4400–4413.
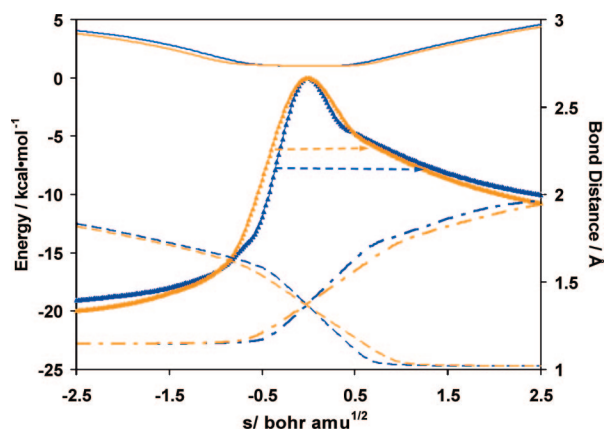(42) Garrett, B. C.; Abusalbi, N.; Kouri, D. J.; Truhlar, D. G. *J. Chem. Phys.* **1985**, *83*, 2252–2258.

Figure 3. Plots of vibrationally adiabatic ground-state potential energy curves (triangles), which are used for obtaining tunneling probabilities, for single configurations in the TSEs of HH (blue) and DH (orange), with their respective representative tunneling energies (horizontal dashed arrows). Also shown are the hydrogen donor−acceptor distances (solid lines) and the lengths of the breaking bonds (dot-dash lines) and forming bonds (dashed lines). Energy and distance units are shown on the left- and right-hand axes, respectively. All of the curves are plotted as a function of the coordinate *s* defined in the text.

at a given energy, followed by a Boltzmann average over energies.[2] Usually, the most important aspect of this approach is that it involves tunneling over a range of donor−acceptor distances. This coupling of the tunneling path to the donor−acceptor distances is similar to the environmentally coupled tunneling model of Kuznetsov and Ultrup[43] in the sense that both methods include a factor that reflects the interplay between donor−acceptor configuration and quantum tunneling. As the system moves along the reaction coordinate, the donor−acceptor distance shortens from ∼2.9 to ∼2.7 Å prior to reaching the RTE configuration and then remains nearly constant at ∼2.7 Å until the hydride transfer has occurred. In the reaction with large curvature, the optimal tunneling path is almost a straight line connecting the reactant and product valleys. Therefore the distance between the donor and acceptor atoms is approximately constant along the tunneling path (see Figure 1 of ref 2).

An example of the isotope-dependent, vibrationally adiabatic ground-state potential energy curve (i.e., the potential energy including the zero-point energy contribution, which is used in calculating the tunneling probability) for one TSE configuration is shown in Figure 3 for each of the isotopic forms HH and DH. This is the effective potential for both ZCT and SCT as well as for LCT and μOMT in the regions near the path termini. As expected, the RTE for DH is closer to the top of the adiabatic energy barrier (5.53 kcal mol^{-1} below the barrier) than that for HH (6.33 kcal mol^{-1} below). The intersections of the RTE with the adiabatic energy barrier (the classical turning points) indicate the structures where the system changes from a classical to a tunneling regime. Although the RTE is isotope-dependent, the average donor−acceptor distances at the RTE (2.73 ± 0.01 Å) are very similar for the four isotopomers. Our results suggest that the reacting moieties first approach by classical activation to a donor−acceptor distance of 2.73 ± 0.01 Å, at which point the hydride tunnels a distance of ∼0.4 Å.

Motion Prior to Tunneling. In the reactants, the rings of the nicotinamide and isoalloxazine moieties are stacked roughly parallel to each other (Figure 2A). Our calculations posit that as the system moves toward a "tunneling-ready" configuration,

the nicotinamide ring rotates to become almost perpendicular to the isoalloxazine ring (Figure 2A), a dynamical change required in order to facilitate the reaction chemistry.[44−47] This is supported by our experimental studies, which showed that NADH binding and the subsequent H transfer can be resolved. The reactant complex behaves as a characteristic charge-transfer (CT) complex formed by π-stacking of the FMN isoalloxazine and NADH nicotinamide rings.[21,48] Our calculations indicate that formation of the TS configuration (Figure 2A) involves loss of π-stacking, and therefore, the TS species would not be expected to be a CT complex. This is consistent with the experimentally observed concomitant loss of the charge-transfer band upon hydride transfer[48] (see below). Additionally, there is no experimentally observed CT complex in the reduced enzyme−NAD$^+$ complex,[48] consistent with the product configuration shown in Figure 2A. It should be noted that the π-stacking interaction between the isoalloxazine ring and the nicotinamide ring is difficult to study quantum mechanically; even the well-established density functional theory (DFT) methods such as B3LYP may not be accurate enough to describe it well. Some DFT methods recently developed by Truhlar and co-workers have demonstrated improved performance on π-stacking interactions compared with other more traditional DFT methods.[49,50] To address this, we plan to compare the structures of the transition state for MR-catalyzed H transfer obtained using different QM methods and their impact on tunneling.

It is possible that the H transfer from NADH to FMN could occur as a proton-coupled electron transfer (PCET) event rather than as a concerted hydride transfer event. The charge transfer band arises due to π-stacking of the FMN isoalloxazine and NADH nicotinamide rings, so if a PCET mechanism operates in MR, then the CT complex would be lost after electron transfer but not after proton transfer. Experimentally we know that (1) the apparent rate of the loss of the charge-transfer complex is identical to the rate of FMN reduction, (2) no FMN semiquinone species is observed during the reductive half-reaction, and (3) there is a considerable KIE on the apparent rate of charge-transfer loss/FMN reduction. Therefore, FMN appears to become reduced in a single two-electron reduction, and this electron transfer is kinetically coupled to H transfer. Thus, if H transfer in MR does occur by PCET, then it does so in a concerted way; the data are inconsistent with a stepwise reaction, where proton transfer is at least partly rate-limiting.

The observed 1° KIE in MR is highly temperature-dependent [Δ(Δ$H^‡$) = 2.1 ± 0.4 kcal mol^{-1}],[20] leading us to suggest previously that the H-transfer reaction coordinate is coupled to a promoting motion in the enzyme that reduces the H-transfer distance.[15,19,20] In the present study, our results suggest two distinct changes in the heavy-atom configuration that reduce the donor−acceptor (C4$_{NADH}$−N5$_{FMN}$) distance. The first (larger) motion involves rotation of the isoalloxazine and nicotinamide rings to form the nearly perpendicular configuration at the TS (Figure 2A). This we can tentatively attribute to a reorganization step. This step is likely to be equilibrated such that the

(43) Kuznetsov, A. M.; Ulstrup, J. *Can. J. Chem.* **1999**, *77*, 1085–1096.

(44) Bruice, T. C. *Chem. Rev.* **2006**, *106*, 3119–3139.

(45) Hammes-Schiffer, S.; Benkovic, S. J. *Annu. Rev. Biochem.* **2006**, *75*, 519–541.

(46) Henzler-Wildman, K.; Kern, D. *Nature* **2007**, *450*, 964–972.

(47) Nagel, Z. D.; Klinman, J. P. *Chem. Rev.* **2006**, *106*, 3095–3118.

(48) Craig, D. H.; Moody, P. C. E.; Bruce, N. C.; Scrutton, N. S. *Biochemistry* **1998**, *37*, 7598–7607.

(49) Zhao, Y.; Truhlar, D. G. *Phys. Chem. Chem. Phys.* **2005**, *7*, 2701–2705.

(50) Dkhissi, A.; Blossey, R. *Chem. Phys. Lett.* **2007**, *439*, 35–39.

experimentally observed CT complex, which is relatively weak in MR, reports only on the fraction of MR−NADH binary complex in the reactant state. The second motion we have observed involves the much smaller (∼0.2 Å) reduction in the C4−N5 distance in the TS complex (Figure 3). This latter motion is likely to be involved in, or a consequence of, the promoting motion. By treating this 0.2 Å change in distance as the root-mean-square displacement (Δr_{rms}) of a harmonic oscillator describing this gating motion,[14,43] we can estimate the frequency (ω) of the oscillating mode using the expression $\Delta r_{rms} = (k_B T/m\omega^2)^{1/2}$, where k_B is Boltzmann's constant. The reduced mass (m) of the gating mode is likely to involve at a minimum both the isoalloxazine and nicotinamide rings ($m \approx$ 80 u), corresponding to an upper limit of ∼50 cm^{-1} on the gating frequency. This frequency is much lower than those reported previously for promoting motions in H-transfer reactions (∼150 cm^{-1} in alcohol dehydrogenase[51] and ∼165 cm^{-1} in aromatic amine dehydrogenase[14]) but consistent with the highly temperature-dependent KIE observed experimentally.

Hydride Transfer in the Deep Tunneling Regime. Our study suggests that over 99% of the hydride transfer reaction from NADH to FMN in MR proceeds via tunneling. This is the first time that such a high degree of tunneling has been calculated for an enzyme-catalyzed hydride transfer reaction, placing the reaction in the so-called deep tunneling regime. Other enzyme reactions that share this extent of tunneling are the proton-tunneling reactions in the two related quinoprotein enzymes aromatic amine dehydrogenase[9] and methylamine dehydrogenase[52,53] and in soybean lipoxygenase;[10] in all of these reactions, the KIE is significantly greater than the semiclassical limit of 7. In contrast, the experimentally measured KIE in MR is less than the semiclassical limit; this is the first example of such a low KIE in a deep tunneling reaction.

Impact on KIE of Substitution at the 1° and 2° Positions. In contrast to computational studies on other systems (alcohol dehydrogenase[6] and dihydrofolate reductase from *Escherichia coli*[17]) using a similar theoretical approach, we observe that isotopic substitution at the primary position has a greater impact on the computed tunneling probability than replacement at the secondary position. On the basis of $\kappa^{\mu OMT}$ values averaged over the TSEs, the KIE decreased by 74% upon replacement of H with D at the 1° position but only by 37% when the equivalent replacement was made at the 2° position. Given the possibility that kinetic complexity impacts the experimental results and the intricacy of the interactions contributing to the free-energy changes along the reaction path, the excellent agreement between the calculated (1.22) and experimental (1.18) 2° KIEs adds credence to our calculations.

Concluding Remarks. It has become widely accepted that quantum-mechanical tunneling plays a significant role in enzyme-catalyzed hydrogen-transfer reactions. Our calculated 1° and 2° KIEs are both in good agreement with the experimental values, adding support to our computed results. Nevertheless, in view of the fact that the experimentally observed KIE lies below the semiclassical limit, the extent to which hydrogen tunneling dominates the hydride-transfer reaction from NADH to FMN in MR (our calculations suggest ∼99% of reaction proceeds via tunneling) was somewhat unexpected. This is the first time that such a deep tunneling reaction, which is an established mechanism in proton tunneling, has been observed for hydride transfer. Our results also suggest that the isotope at the 1° position has a substantial impact on the dominant tunneling mechanism but the one at the 2° position does not. With protium in the 1° position, LCT dominates, whereas with deuterium, SCT dominates. Additionally, our study is consistent with tunneling being preceded by reorganization: in the reactants, the rings of the nicotinamide and isoalloxazine moieties are stacked roughly parallel to each other, and as the system moves toward a "tunneling-ready" configuration, the nicotinamide ring rotates to become almost perpendicular to the isoalloxazine ring.

Supporting Information Available: Tunneling factors (κ), dynamic recrossing factors (Γ), and the overall transmission coefficient (γ) at 25 °C (Table S1); reaction rate constants and KIEs at 25 °C (Table S2); tunneling factors (κ) calculated at 25 °C using the ZCT, SCT, LCT, and μOMT methods (Table S3); and complete refs 28 and 34. This material is available free of charge via the Internet at http://pubs.acs.org.

JA800471F

(51) Mincer, J. S.; Schwartz, S. D. *J. Phys. Chem. B* **2003**, *107*, 366–371.
(52) Faulder, P. F.; Tresadern, G.; Chohan, K. K.; Scrutton, N. S.; Sutcliffe, M. J.; Hillier, I. H.; Burton, N. A. *J. Am. Chem. Soc.* **2001**, *123*, 8604–8605.
(53) Ranaghan, K. E.; Masgrau, L.; Scrutton, N. S.; Sutcliffe, M. J.; Mulholland, A. J. *ChemPhysChem* **2007**, *8*, 1816–1835.
(54) Garcia-Viloca, M.; Alhambra, C.; Truhlar, D. G.; Gao, J. *J. Chem. Phys.* **2001**, 9953–9958.